AD-A115 538 AIR FORCE INST OF TECH WRIGHT-PATTERSON AFB OH SCHOO--ETC F/G 20/3
FREE SPACE ANALYSIS OF THE SCATTERED ELECTROMAGNETIC FIELDS AS --ETC(U)
DEC 81 D L TOMCZYK
UNCLASSIFIED AFIT/GE/EE/81D-60 NL

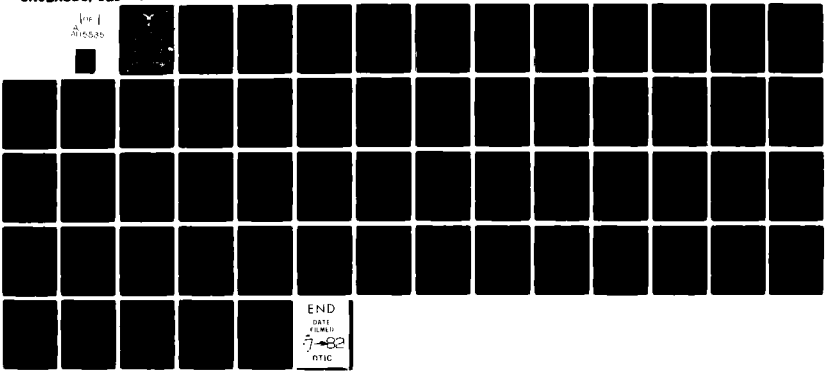

END
DATE FILMED
7-82
DTIC

DEPARTMENT OF THE AIR FORCE

AIR UNIVERSITY (ATC)

AIR FORCE INSTITUTE OF TECHNOLOGY

Wright-Patterson Air Force Base, Ohio

AFIT/GE/EE/81D-60

FREE SPACE ANALYSIS OF THE SCATTERED ELECTROMAGNETIC FIELDS AS A DIPOLE APPROACHES A LEAKY COAXIAL CABLE

THESIS

AFIT/GE/EE/81D-60 Daryl L. Tomczyk
1st Lt. USAF

Approved for public release; distribution unlimited.

AFIT/GE/EE/81D-60

FREE SPACE ANALYSIS OF THE SCATTERED ELECTROMAGNETIC FIELDS AS A DIPOLE APPROACHES A LEAKY COAXIAL CABLE

THESIS

Presented to the Faculty of the School of Engineering
of the Air Force Institute of Technology
Air University
in Partial Fulfillment of the
Requirements for the Degree of
Master of Science

by

Daryl L. Tomczyk, B.S.E.E.
1Lt USAF
Graduate Electrical Engineering

December 1981

Approved for public release; distribution unlimited.

Acknowledgements

I wish to express my appreciation to Dr. J. Leon Poirier of the Rome Air Development Center (Hanscom AFB, MA) for this topic and also for his support and encouragement. Thanks is also due my readers, Major August Golden and Professor Raymond Potter, for their help and positive feedback. Most of all I wish to thank my thesis advisor, Captain Thomas Johnson, for his guidance, patience and continual encouragement.

Finally, I am indebted the most to my wife, Eileen, for her understanding and allowing me to sacrifice our family life and complete my work at AFIT.

Daryl L. Tomczyk

This thesis typed by Maripat Meer

Contents

Acknowledgements ii

List of Figures iv

Notation v

Abstract vii

I. Introduction 1

- Background 1
- Problem 2
- Assumptions 4
- Approach and Presentation 5

II. Development of Theory 7

- Non-Plane Wave Incident on a Dipole 9
- Development of the Induced Dipole Current . . . 13
  - The Pocklington Integral 14
  - The Method of Moments 21
- Fields at the Antenna 25
- Voltage at the Antenna 27

III. Results 28

- Theoretically Derived Results 28
- Review of Poirier Report 34
- Comparison of Results 35

IV. Conclusions and Recommendations 38

- Conclusions 38
- Recommendations 39

Bibliography 40

Appendix A: Developed Computer Program 42

VITA 48

List of Figures

Figure		Page
2.1	Dipole Orientation	10
2.2	Incident Electric Field Variation Across the Dipole for Two Intruder Distances, D=0.05 and D=1.25 Wavelengths	12
2.3	Induced Current Distribution for Two Intruder Distances, D=0.05 and D=1.25 Wavelengths	15
2.4	Dipole in Free Space	16
3.1	Power Decay Rate for the Coaxial and 'Goubau' Modes.	29
3.2	Normalized Received Power Variation as an Intruder Moves Along a Radial Path	31
3.3	Normalized Received Voltage Variation as an Intruder Moves Along a Radial Path	32
3.4	Normalized Received Power Variation as an Intruder Moves Along a Radial Path (For the Case when Ambient Power = 37% Maximum Intruder Scattered Power)	33
3.5	Computed Variation of Received Power as an Intruder Moves Along a Radial Path, λ_0=4 meters.	36

Notation

Roman Letter Symbols

a	Radius of dipole
$\overline{A}$	Magnetic vector potential
D	Distance from cable to intruder
$\overline{E}$	Electric field
f	Frequency
$F_n(\ )$	Pulse expansion functions
$G(\ )$	Free space scalar Green's function
h_0	Transverse wave number
H_θ	Scalar Magnetic field, θ component
$H^{(1)}(\ )$	Hankel function of the first kind
$\overline{I}$	Line current
$\overline{J}$	Surface current density
k_0	Free space propagation constant
$K_1(\ )$	Modified Bessel function of the second kind, order one
L	Length of dipole
N	Number of sub-dipoles
t	Time
v	Phase velocity
X	Distance from cable to receiving antenna (12 wavelengths)
Δz_n	Length of each sub-dipole

Notation

Greek Letter Symbols

α	Angle of incidence on dipole
β	Propagation constant
γ_n	Angle of incidence on receive antenna, from dipole
ε	Relative permittivity
ε_0	Free space permittivity
η_0	Free space characteristic impedence
θ	Angle of departure from dipole
λ	Wavelength
μ	Relative permeability
μ_0	Free space permeability
ρ	Distance
σ	Conductivity
ϕ	Angle of incidence on receive antenna, from cable
Φ	Scalar potent ·l
ω	Angular frequency

Abstract

The free space interaction of the near zone electromagnetic fields external to a leaky coaxial cable and a moving dipole is investigated. The method of moments and the equivalence principle are used to find the currents on the dipole and the electromagnetic fields scattered from the dipole. Finally, the overall interaction between these two fields is determined by superposition. The theoretically derived results are then compared with experimental measurements.

The findings of this report indicate that exact results are not obtained with a free space analysis; therefore, further work involving electronic intruder detection analysis should include the effects of the earth-air interface.

FREE SPACE ANALYSIS OF THE SCATTERED ELECTROMAGNETIC FIELDS AS A DIPOLE APPROACHES A LEAKY COAXIAL CABLE

I. INTRODUCTION

1.1 Background

The USAF, DOD and many other government agencies are investigating the use of electronic intruder detection systems for protection of critical permanent and semi-permanent areas, such as MX sites, nuclear power plants, forward located air strips, and other high value resources. One such system is the Single Wire Individual Resource Protection Sensor (SWIRPS). The SWIRPS system consists of a single leaky coaxial cable, which encircles the resource to be protected, and a centrally-located monopole receiving antenna. The leaky coaxial cable allows a small portion of the RF energy travelling inside the cable to "leak" out, either through gaps in a loose braid or through periodic slots cut in a solid outer conductor, and propagate along the outside of the cable. As an intruder approaches the leaky coaxial cable, which acts as a waveguiding structure, the Electromagnetic (EM) fields are disturbed, thereby changing the received signal at the monopole. When the

change in the received signal is sufficiently large a detection is declared; therefore, it is the interaction of an intruder with the external EM field that allows detection.

1.2 Problem

The intent of this thesis is to study the interaction between a radially approaching intruder and the EM fields created by the leaky coaxial cable, so that the resulting EM fields at the receiving antenna can be determined. In order to scope down the problem to a workable and more general case, only the plane containing the intruder, the coaxial cable, and the receiving antenna will be examined.

Before any analysis of the interaction between the EM fields and the intruder can be made, the propagation characteristics of a leaky coaxial cable must be known. A solution for lossless leaky coaxial cables in free space has been obtained by Fernandes (Ref 4). His solution is based on the concept of surface transfer impedence and shows the existance of two propagating modes, the coaxial and the 'Goubau' modes. Fernandes indicates that the coaxial mode exists when the cable is excited in the normal coaxial manner; if however, the cable is excited as a solid wire, the 'Goubau' mode exists. The coaxial mode has the majority of its energy propagating inside the cable, is little affected by the outside medium, and thus is of minimal help

in intruder detection. The 'Goubau' (or surface attached) mode however, has a bound, non-radiating, radially evanescent field with the majority of its energy propagating outside the cable, and is therefore very dependent upon the outside environment. The radial decay, or attenuation, of the 'Goubau' mode, though highly dependent on the frequency of operation and the inside dielectric permittivity (Ref 4:259), is also affected by the outside environmental conditions, such as snow, rain, ice, etc (Ref 13:135), which are changing conditions that cannot be designed in or permanently fixed. Future work should investigate the effect of the cable located on or in an earth model, which could also be used to predict any detection degradation due to changing environmental conditions.

Some initial analysis of the intruder/leaky-cable interaction have been performed (Ref 8:7-17, Ref 10); wherein the intruder was simply modeled as a scattering point source, therefore, no effects due to size or orientation could be seen. As an obvious continuation of the previous works, this thesis will model the intruder as a dipole thereby making it possible to determine the effects of intruder orientation. The vertical or standing intruder is the only orientation considered herein. The effects of a non-plane wave incident upon a dipole must be developed since the intruder-dipole model is located in the near field region of the leaky coaxial cable.

The SWIRPS system being considered has the cable located on the surface of the earth; thus, the leaky coaxial cable, the receiving antenna, and the intruder are on the same base plane. Also, since experimental measurements indicate that the zone of detection is less than a wavelength (Ref 11:18), the intruder will only be considered to move within ±two wavelengths of the coaxial cable.

1.3 Assumptions

An analysis of this effort will be made making the following assumptions:

1. All analysis will be performed in free space. This assumption is being made since the only form available for the external EM fields from a leaky coaxial cable are for the cable located in free space, or for the cable located within a mine shaft. It was decided that the free space analysis would be more appropriate to this study. In addition, the skin depth for dry clay soil at 10 MHz (Ref 16:314) was calculated to be in the range of 85 meters, thus indicating minimal effect of the earth-air interface since the radial electric field normally decays at a much faster rate.

2. The leaky coaxial cable is considered to be lossless, infinitely long, and straight.

3. The intruder will be modeled as a perfectly conducting thin cylinder (approaching a dipole). The

intruder dipole model will be 0.355 wavelengths in length with the radius being much less than a wavelength; since the operating frequency is 60MHz (λ=5 meters), this corresponds to a 5'-10" intruder.

1.4 Approach and Presentation.

The theory is developed in Chapter II using the following approach to determine the interaction of a moving intruder with the EM fields created by the leaky coaxial cable. First, the field induced currents on the intruder must be determined; this will be accomplished via the method of moments. The method of moments being a technique for solving an integral equation, which can be readily implemented on a computer. Once an algorithm is developed to determine the field induced currents on the intruder, the electric field at the receiving antenna can be determined by summing the source field and the intruder scattered field. Finally, the interaction of the leaky coaxial EM fields and the intruder (with position) can then be obtained. Chapter II also contains sample numerical results giving the incident field along the dipole and the resulting currents induced on the dipole for two selected positions.

Chapter III presents the results obtained from the developed computer program (Appendix A) using the approach given in Chapter II. The received power at the receiving antenna as a function of intruder distance from the cable is

given for two ambient power levels. These results are then compared to those calculated and experimentally obtained by Poirier (Ref 8).

The conclusions and recommendations are presented in Chapter IV.

II. DEVELOPMENT OF THEORY

Loose braid or 'leaky' coaxial cables have been studied primarily for the purposes of communications within mine shafts. The theory developed in these cases is not applicable to this study because the mine shaft problem imposes a different boundary condition on the field development; that is, for the case of the mine shaft, the fields are such that they must go to zero at the tunnel walls, as opposed to going to zero at infinity.

The propagation characteristics for the special case of a loose braid coaxial cable in free space has been determined by Fernandes. His solution, which is based on the surface transfer impedence concept, shows the existence of two propagating modes, the coaxial mode, and the 'Goubau' mode. Fernandes describes the fields external to the leaky cable, for either mode, as

$$E_z = A_0 H_0^{(1)}(jh_0\rho)\exp(-j\beta z)\exp(j\omega t) \tag{2.1}$$

$$E_\rho = A_0 \frac{\beta}{h_0} H_1^{(1)}(jh_0\rho)\exp(-j\beta z)\exp(j\omega t) \tag{2.2}$$

$$H_\theta = A_0 \frac{k_0^2}{\omega\mu_0 h_0} H_1^{(1)}(jh_0\rho)\exp(-j\beta z)\exp(j\omega t) \tag{2.3}$$

where $H^{(1)}(\ )$ are Hankel functions of the first kind for order zero and one, β is the propagation constant (which is determined by the mode selected), k_0 is the free space propagation constant, h_0 is the transverse wave number defined as $h_0^2=\beta^2-k_0^2$, and A_0 is a constant assumed to be unity hereafter (Ref 4:256).

Since the problem analyzed in this study is only for a particular cut of an infinitely long, lossless, and straight cable, the phase variation arising from the $e^{-j\beta z}$ term is constant for any particular 'z', and thus can be ignored. Also, realize that for the case of a lossless line, as considered herein, h_0 is always a real number, and therefore by using the relations between solutions for Hankel functions and the Modified Bessel functions of tne second kind, (Ref 1:375), the expressions for E_ρ and H_θ become

$$E_\rho = \frac{\beta}{h_0}\left\{-\frac{2}{\pi}K_1(h_0\rho)\right\} \tag{2.4}$$

$$H_\theta = \frac{k_0^2}{\omega\mu_0 h_0}\left\{-\frac{2}{\pi}K_1(h_0\rho)\right\} \tag{2.5}$$

Experimental measurements indicate the existence of two interfering waves, propagating in the z direction, external

to the leaky cable (Ref 9); this implies that a form of the 'Goubau' mode is excited by the coaxial mode fields that have 'leaked' to the outside. Based on the above assumption, the field structure used in this study is of the form

$$E_\rho = E_\rho(\beta_1) + C\, E_\rho(\beta_2) \qquad (2.6)$$

where β_1 is the propagation constant for the coaxial mode, β_2 is the propagation constant for the 'Goubau' mode, and C is a constant assumed to be unity hereafter. The values for β_1 and β_2 are calculated using the relationship $\beta=\frac{2\pi f}{v}$, where v is the phase velocity and f is the frequency of operation. Experimental measurements of β_1 and β_2 have been made at 75 MHz (Ref 8:23); thus, the values of β_1 and β_2 at 60 MHz can be calculated as β_1 =1.72 rads/m and β_2=1.32 rads/m .

2.1 Non-Plane Wave Incidence on a Dipole

The moving dipole, as shown in Figure 2.1, will interact with the vertical component of the electric field described by equation 2.6. The close proximity of the dipole to the leaky coaxial cable results in a significant variation of the electric field across the length of the dipole. In order to determine the excitation of the dipole, we must consider the dipole as being broken into N equal sub-dipoles, or segments, where the length of each segment,

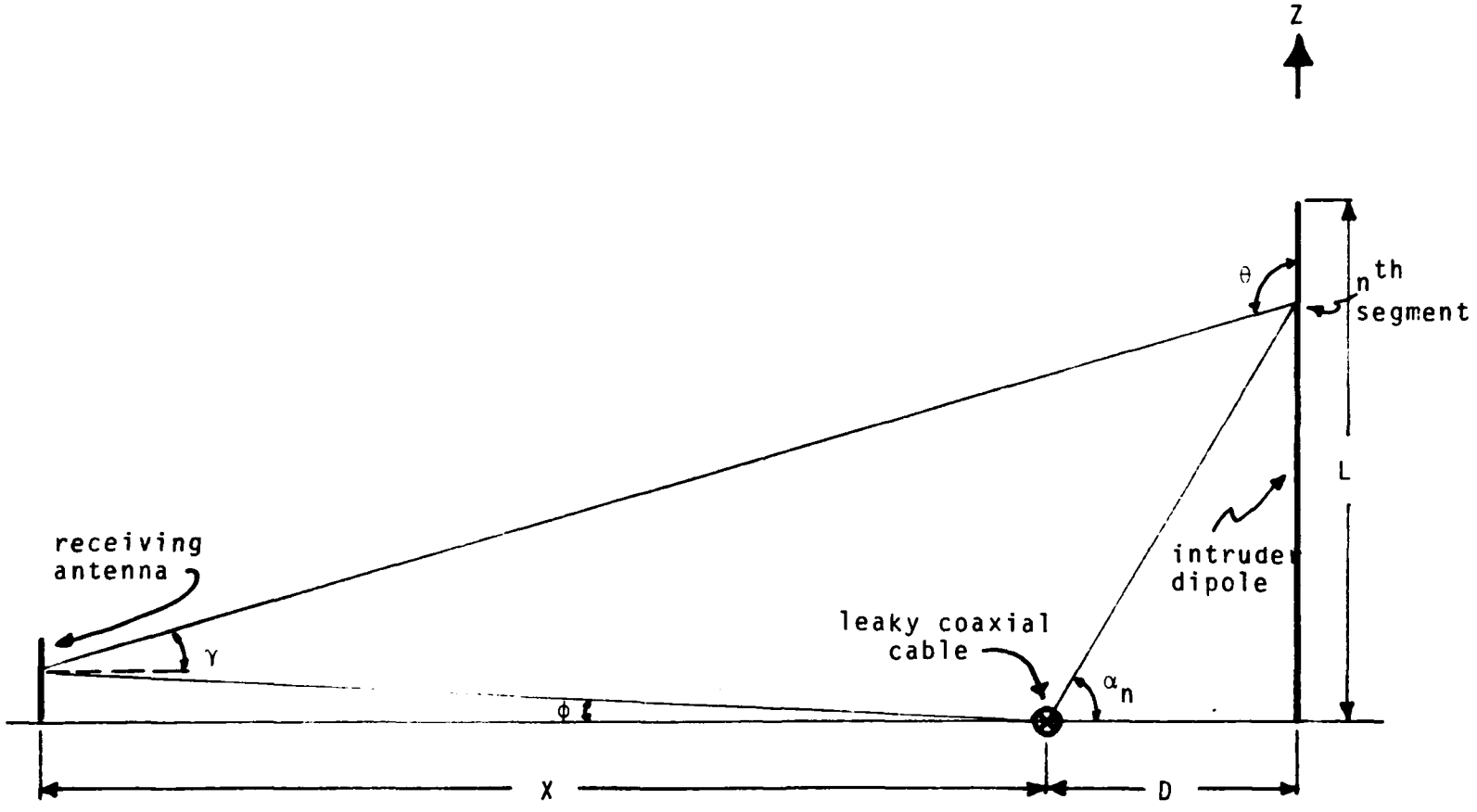

Figure 2.1 Dipole Orientation

L/N, is such that the electric field variation across it is minimal. Also, assume that the electric field present at the center of each segment is also the electric field that exists over the entire segment. The dipole is now being viewed as an array of N dipoles, each being excited by an incident electric field which can be described as

$$E_n^i = [E_\rho(\beta_1) + E_\rho(\beta_2)]\sin(\alpha_n) \tag{2.7}$$

where E_n^i is the vertical component of the incident electric field at the n^{th} element and α_n is the angle of incidence at the n^{th} element, n being 1 at the bottom and N at the top of the dipole. The angle of incidence, α_n , is a function of the dipoles horizontal distance from the cable, D, as well as the segment being excited, n , and is given by

$$\alpha_n = \arctan\left[\frac{\frac{L}{N}(n-\frac{1}{2})}{D}\right] \tag{2.8}$$

Thus, the amount of coupling at each sub-dipole or segment is seen to be dependent upon the location of the dipole and also the location of the segment being excited. Figure 2.2 is a plot of the magnitude of the incident electric field by

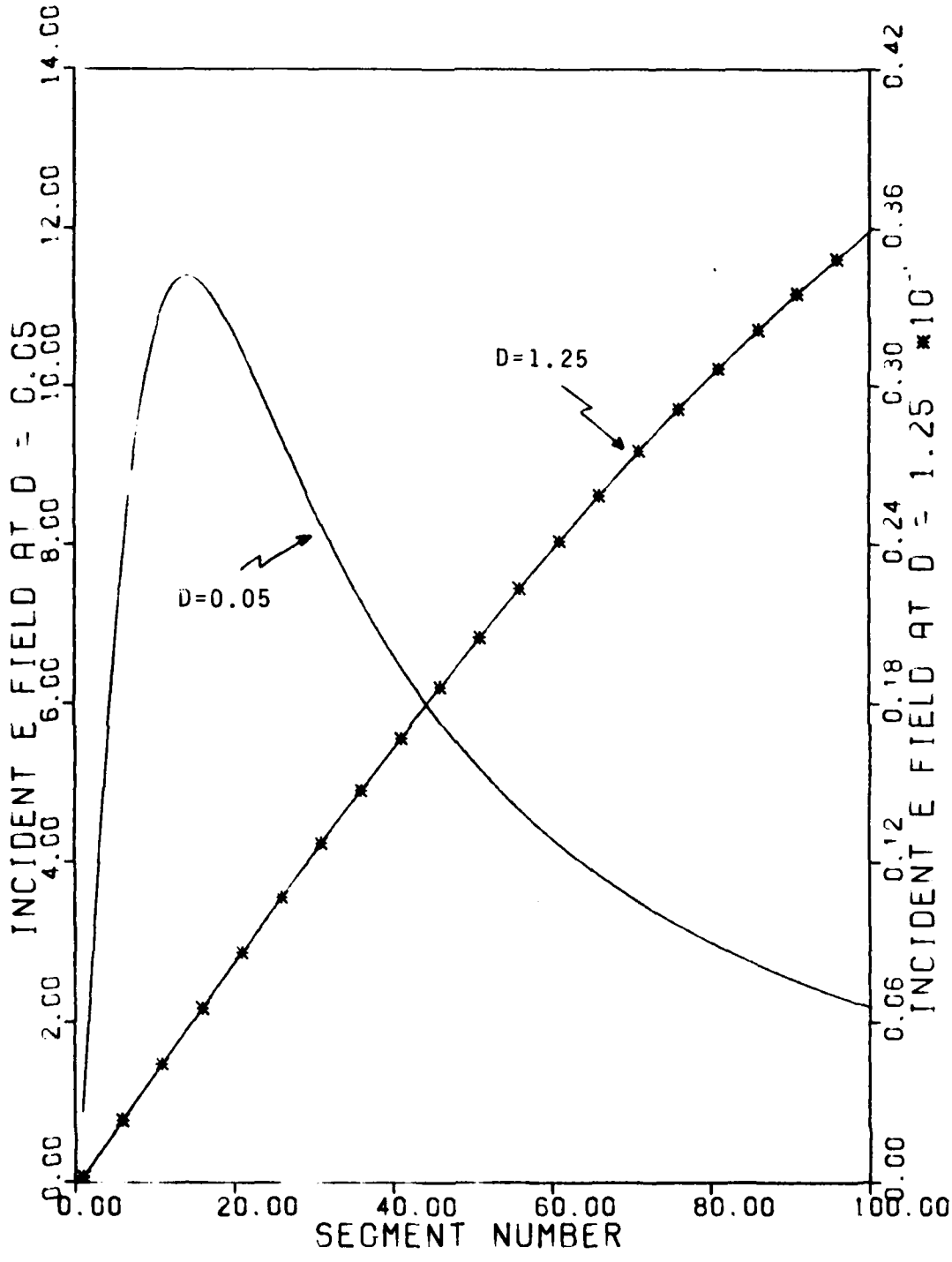

Figure 2.2 Incident Electric Field Variation Across the Dipole for Two Intruder Distances, D=0.05 and D=1.25 Wavelengths. (Note: The units of the electric field are volts/wavelength).

segment for two distances from the coaxial cable, D=0.05 and D=1.25 wavelengths. For small distances, as shown in the D=0.05 curve, the variation of the sine function overshadows the Bessel function variation.

Now, in order to determine the induced dipole current, the method of moments will be used; it is therefore convenient that the incident electric field has already been determined at each of the N segments.

2.2 Development of the Induced Dipole Current

The development presented in this section is a redevelopment of the pertinent sections of chapter 7, Ref 14. The induced dipole current gives rise to a scattered electric field, $\overline{E}^s$; so, in order to obtain an expression for $\overline{E}^s$, the induced dipole current will be determined using the method of moments. The method of moments is a computer oriented technique which enables one to solve an integral equation, in this case, Pocklington's Integral Equation, in terms of the desired dipole current. The first step is to approximate the integral equation by a set of linear algebraic equations with the source induced current on the dipole being the unknown. The dipole is then divided into N segments with each segment given an unknown current function; for this study, pulse function currents of unknown amplitude will be used as the unknown current functions because of the greatly simplified integration associated

with their use. The problem is now expressed in the form $V=ZI$, where V represents the incident electric field, $\overline{E}^i$; Z is a form of an impedence matrix; and, I is the unknown current distribution. An expression for the unknown current distribution, in terms of the source or incident field, can now be obtained using a matrix inversion technique. Since pulse function currents are used, the unknown current distribution is only approximated; but if the width of the pulse functions is much less than a wavelength, a good approximation of the dipole current distribution is obtained by curve fitting the values of the pulses. Also, with this form of excitation, the induced current had a linear 6^o phase variation across the dipole. Figure 2.3 is a plot of the induced current by segment for the two incident electric fields plotted in Figure 2.2; note that while the induced current distribution maintains the same basic shape, the maximum level is skewed towards the segment which had maximum incident electric field.

2.2.1 The Pocklington Integral. Assume a dipole of length L and radius a is located in free space, as shown in Figure 2.4. Also, assume that the radius of the dipole is much less than the free space wavelength and the dipole length L; it is then reasonable to assume that the induced dipole current has only a $\hat{z}$ component. In this case, the Lorentz Condition $\nabla\cdot\overline{A}= -j\omega\mu_0\epsilon_0\Phi$ will reduce to

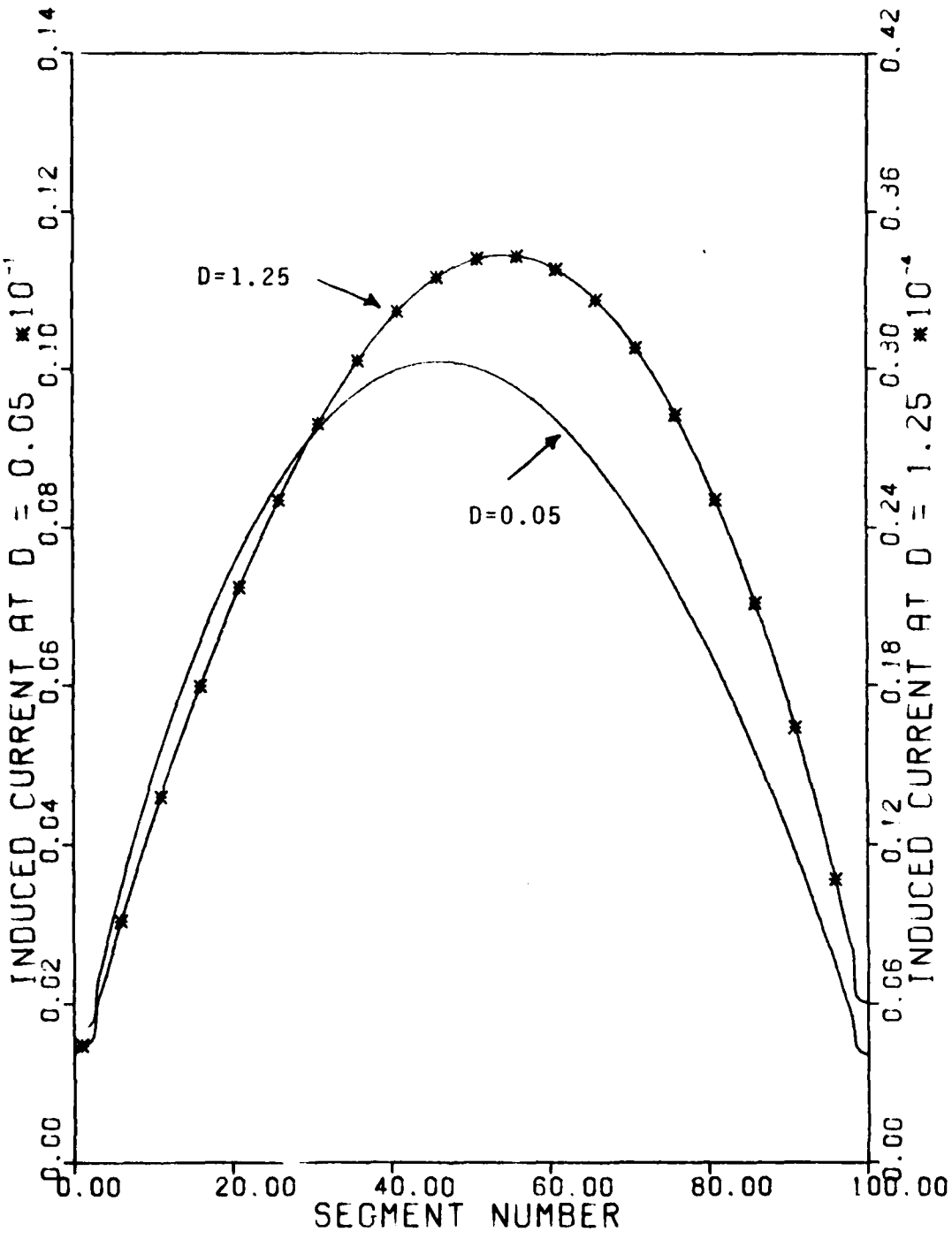

Figure 2.3 Induced Current Distribution for Two Intruder Distances, D=0.05 and D=1.25 Wavelengths. (Note: The units of the induced current are amps/wavelength).

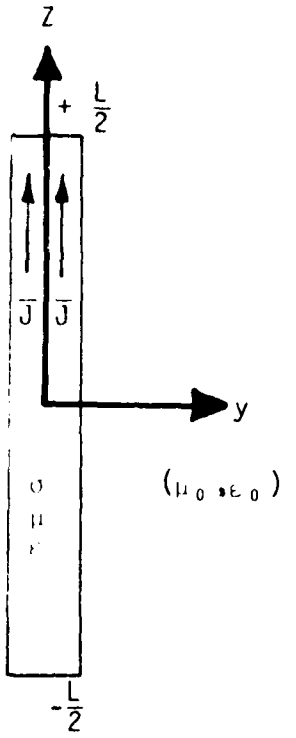

Figure 2.4 Dipole in Free Space.

$$\frac{\partial A_z}{\partial z} = -j\omega\mu_0\varepsilon_0\Phi \tag{2.9}$$

where Φ is the scalar potential and A_z is the $\hat{z}$ directed component of the magnetic vector potential.

Now, writing Maxwell's Equation in terms of the magnetic potential $\bar{A}$ as

$$\bar{E} = -j\omega\bar{A} + \frac{\nabla V \cdot \bar{A}}{j\omega\mu_0\varepsilon_0} \tag{2.10}$$

and, since $\bar{A} = \hat{z} A_z$, equation 2.10 can be reduced using the relationship of equation 2.9 to

$$E_z = -j\omega A_z - \frac{\partial \Phi}{\partial z} \tag{2.11}$$

From equation 2.9 solve for $\frac{\partial \Phi}{\partial z}$ as

$$\frac{\partial \Phi}{\partial z} = - \frac{1}{j\omega \mu_0 \varepsilon_0} \frac{\partial^2 A_z}{\partial z^2} \tag{2.12}$$

Now, substituting equation 2.12 into 2.11 yields

$$E_z = \frac{1}{j\omega \mu_0 \varepsilon_0} \left[\frac{\partial^2 A_z}{\partial z^2} + k_0{}^2 A_z \right] \tag{2.13}$$

where $k_0 = \omega \sqrt{\mu_0 \varepsilon_0}$, the free space propagation constant. The magnetic vector potential, $\bar{A}(\bar{r})$, arising from a volumetric current density, $\bar{J}(\bar{r}')$, can be obtained from

$$\bar{A}(\bar{r}) = \mu_0 \int_{V'} \bar{J}(\bar{r}') \frac{e^{-jk_0 R}}{4\pi R} \, dV' \tag{2.14}$$

where R is the distance from the observation point (x,y,z) to the source point (x',y',z') and is given by

$$R = \sqrt{(x-x')^2+(y-y')^2+(z-z')^2} \tag{2.15}$$

Noting that the free space scalar Green's function is expressed as

$$G(\bar{r},\bar{r}') = \frac{e^{-jk_0R}}{4\pi R} \tag{2.16}$$

and that the volumetric current density only has a $\hat{z}$ component, that is $\bar{J}(\bar{r}')=\hat{z}J_z(\bar{r}')$, equation 2.13 can now be written as

$$E_z = \frac{1}{j\omega\epsilon_0}\int_{V'}\left[\frac{\partial^2}{\partial z^2}G(\bar{r},\bar{r}')+k_0^2G(\bar{r},\bar{r}')\right]J_z(\bar{r}')dV' \tag{2.17}$$

This volume integral can be further reduced to a line integral by making the following assumptions:

1. The current is confined to the surface of the dipole; this is true for infinite conductivity, and approximately true for good conducting material;

2. The observation point is chosen to be a point on the z axis, thus reducing equation 2.15 to

$$R = \sqrt{(z-z')^2 + a^2} \tag{2.18}$$

3. The current is uniform with respect to ϕ', $a<<\lambda$. Thus we can write equation 2.17 in line integral form as

$$E_z = \frac{1}{j\omega\epsilon_0} \int_{-\frac{L}{2}}^{+\frac{L}{2}} \left[\frac{\partial^2}{\partial z^2} G(z,z') + k_0^2 G(z,z')\right] I(z')dz' \tag{2.19}$$

This equation states that the induced current can be written as a line current located a distance a from the observation point; note that a can approach zero but cannot go entirely to zero. By the use of the Equivalence Principle (Ref 5:104-110), E_z in equation 2.19 can be written as E_z^s, the free space field radiated by the equivalent current $I(z')$. Also, since a perfect conductor was assumed, there will be no losses at the dipole. Therefore, the incident field, E_z^i, which created the induced current $I(z')$, and the scattered field, E_z^s, resulting from $I(z')$, must be related at the

dipole so that the total electric field is zero, that is

$$E_z = E_z^i + E_z^s = 0 \tag{2.20}$$

or,

$$E_z^i = -E_z^s \tag{2.21}$$

Thus we can write equation 2.19, the Pocklington Integral Equation, as

$$-E_z^i = \frac{1}{j\omega\epsilon_0} \int_{-\frac{L}{2}}^{+\frac{L}{2}} \left[\frac{\partial^2}{\partial z^2} G(z,z') + k_0^2 G(z,z')\right] I(z')dz' \tag{2.22}$$

Equation 2.22 can be rewritten as

$$E_z^s = \frac{1}{4\pi j\omega\epsilon_0} \int_{-\frac{L}{2}}^{+\frac{L}{2}} \frac{e^{-jk_0R}}{R^5} \left[(1+jk_0R)(2R^2-3a^2)\right. \tag{2.23}$$

$$\left. +k_0^2R^2a^2\right] I(z')dz'$$

2.2.2 The Method of Moments. A specific form of the method of moments is developed and used herein; this form being the point matching technique using pulse expansion functions.

The dipole is divided into N segments, each of length $\Delta z_n' = L/N$, with each segment assumed to have an unknown constant current. A more accurate representation of $I(z')$ can be obtained by increasing the number of segments, thereby tending to smooth out the stairstep approximation; in general N cannot be made arbitrarily large due to finite word length in the computer, leading to numerical instability. With the above assumption, we can write the unknown current distribution as

$$I(z') = \sum_{n=1}^{N} I_n F_n(z') \tag{2.24}$$

where I_n is the complex expansion coefficient of the n^{th} segment and $F_n(z')$ is the pulse expansion function, defined as

$$F_n(z') = \begin{cases} 1 \text{ ; if } z' \text{ is in } \Delta z_n' \\ 0 \text{ ; elsewhere} \end{cases} \tag{2.25}$$

Also, for notational brevity, let us define

$$K(z,z') = \frac{1}{j\omega\varepsilon_0}\left[\frac{\partial^2 G(z,z')}{\partial z^2} + k_0^2 G(z,z')\right] \qquad (2.26)$$

Designating the center point of the particular segment being solved for as z_m , the scattered field arising from the m^{th} segment can be written as

$$E_z^s(z_m) = \int_{-\frac{L}{2}}^{+\frac{L}{2}} \sum_{n=1}^{N} I_n F_n(z') K(z_m,z') dz' \qquad (2.27)$$

If we now use the definition of $F_n(z')$, we can reduce equation 2.27 to

$$E_z^s(z_m) = \sum_{n=1}^{N} I_n \int_{\Delta z_n'} K(z_m,z') dz' \qquad (2.28)$$

and, if we let $f(z_m, z_n') = \int_{\Delta z_n'} K(z_m, z_n')\, dz'$ we have

$$E_z^s(z_m) = I_1\, f(z_m, z_1') + I_2\, f(z_m, z_2') + \cdots + I_N\, f(z_m, z_N') \tag{2.29}$$

In order to solve equation 2.22 at the m^{th} segment, we must have the sum of the scattered fields from all N segments plus the incident field at z_m set equal to zero. We can therefore write N independent equations with the only unknowns being the N I_n's .
The resulting N independent equations being

$$\begin{aligned}
-E_z^i(z_1) &= I_1 f(z_1, z_1') + I_2 f(z_1, z_2') + \cdots + I_N f(z_1, z_N') \\
-E_z^i(z_2) &= I_1 f(z_2, z_1') + \cdots + I_N f(z_2, z_N') \\
&\vdots \\
-E_z^i(z_N) &= I_1 f(z_N, z_1') + \cdots + I_N f(z_N, z_N')
\end{aligned} \tag{2.30}$$

These equations can be written more conveniently in matrix notation as

$$\begin{bmatrix} -E_z^i(z_1) \\ -E_z^i(z_2) \\ \vdots \\ -E_z^i(z_N) \end{bmatrix} = \begin{bmatrix} f(z_1,z_1') & f(z_1,z_2') & \cdots & f(z_1,z_N') \\ f(z_2,z_1') & f(z_2,z_2') & \cdots & \\ \vdots & \vdots & & \vdots \\ f(z_N,z_1') & & & f(z_N,z_N') \end{bmatrix} \begin{bmatrix} I_1 \\ I_2 \\ \vdots \\ I_N \end{bmatrix} \tag{2.31}$$

And in abbreviated form as

$$[V_m] = [Z_{mn}][I_n] \tag{2.32}$$

where $V_m = -E_z^i(z_m)$, and $Z_{mn} = f(z_m,z_n')$ the impedence matrix which was calculated using Simpson's Rule. As was noted earlier, the purpose of this procedure is to solve for the I_n's ; therefore, if we premultiply equation 2.32 by $[Z_{mn}]^{-1}$ we obtain

$$[I_n] = [Z_{mn}]^{-1}[V_m] \tag{2.33}$$

Since a thin dipole is being used in this analysis, the impedence matrix $[Z_{mn}]$ will be Toeplitz (Ref 12:205);

therefore, only one row of the matrix need be determined. $[Z_{mn}]^{-1}$ can then be determined using a Toeplitz inversion routine. Such an inversion routine, SUBPROGRAM TOPIN, was generated by modifying SUBPROGRAM TPLZ (Ref 14:579-81), see Appendix A.

2.3 Fields at the Antenna

The electric field present at the receiving antenna is the superposition of the field received directly from the leaky coaxial cable and the field that is radiated by each of the N sub-dipoles.

The field received directly from the leaky coaxial cable can be simply calculated using the vertical component of the electric field as described by equation 2.6. This received field is given by

$$E^i = [E(\beta_1) + E(\beta_2)] \sin(\phi) \tag{2.34}$$

where ϕ is the angle of incidence, see Figure 2.1.

The field received from the N sub-dipoles is found by examining each sub-dipole separately. Knowing that the current has only a $\hat{z}$ component, and that each segment is small enough so that it appears to be a point source of amplitude $I_n(\frac{L}{N})$, solution of the Helmholtz equation yields

$$A_n(r) = I_n \frac{L}{N} \frac{\exp(-jk_0 r)}{4\pi r} \tag{2.35}$$

where r is the distance from the n^{th} sub-dipole to the receiving antenna. Now, by using Maxwell's equations and the assumption that $r>>\lambda$, we can approximate the electric field at the receiving antenna, from the n^{th} segment, as

$$E_n = I_n \frac{L}{N} \frac{e^{-jk_0 r}}{r} \left(j\frac{\eta_0}{2\lambda}\right) \sin(\theta) \tag{2.36}$$

where θ is the angle as measured from the positive z-axis, and η_0 is the free space characteristic impedence (Ref 5:78-9). Consequently, the electric field at the receiving antenna from the N sub-dipoles will be

$$E = \sum_{n=1}^{N} E_n \sin(\gamma_n) \tag{2.37}$$

or

$$E = j\frac{\eta_0}{2\lambda}\frac{L}{N}\sin(\theta)\sum_{n=1}^{N} I_n e^{-jk_0 r}\sin(\gamma_n) \qquad (2.38)$$

where γ_n is the angle of incidence of the electric field radiated from the n^{th} sub-dipole.

2.4 Voltage at the Antenna

The receiving antenna was arbitrarily chosen to be 0.5 meters, or 0.1 wavelengths, in length. Since this antenna is located in the far field of the ambient and intruder scattered fields, there were no non linear spatial effects and the antenna was considered to act as an ordinary antenna. The relative voltage was found by comparing the received field strengths.

III. RESULTS

This chapter presents the theoretically derived results and compares them with those calculated and experimentally obtained by Poirier (Ref 8).

3.1 Theoretically Derived Results

It was observed that the electric field received directly from the coaxial cable, equation 2.34, is negligible when compared to the electric field which is scattered from the intruder-dipole, equation 2.38. This can be explained by examining the rate of decay of the two field components. *Figure* 3.1 *is a plot of the radiated power versus distance for both the coaxial mode and the 'Goubau' mode;* a $\frac{1}{\rho^2}$ decay rate is also plotted as a reference. Examination of this figure shows that for $\rho>0.5$ meters, the power begins to fall off sharply from the $\frac{1}{\rho^2}$ rate, with the rate of decay being dominated by the exponential behavior of the Bessel function. The electric field from the coaxial cable is a non-radiating field whose decay is dominated by $e^{-\rho}$; where as, the field scattered from the dipole is a radiated field and decays as $\frac{1}{\rho}$. The field received from the coaxial cable was calculated to be approximately 800 dB down from the field scattered from the dipole, for the case when the receiving antenna is located

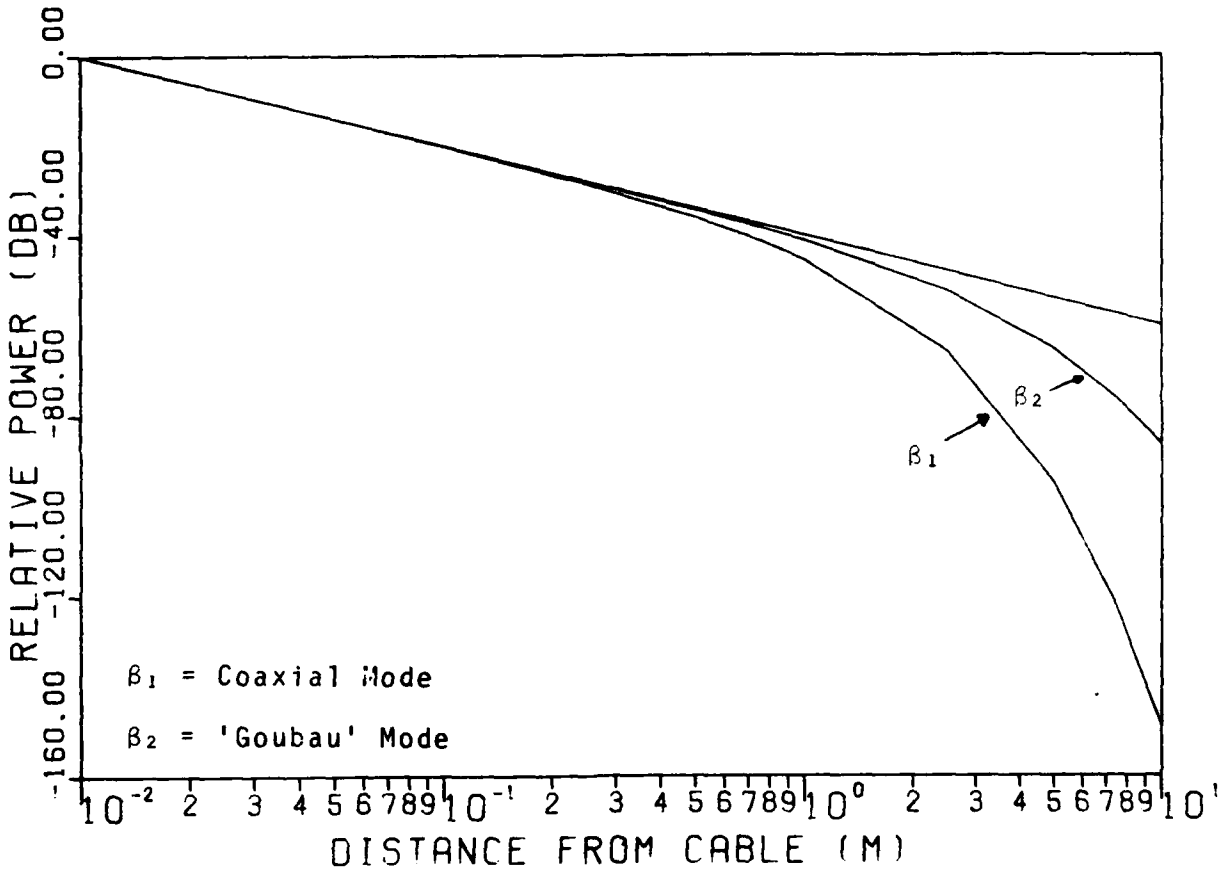

Figure 3.1 Power Decay Rate for the Coaxial and 'Goubau' Modes. The Straight Line is a $1/\rho^2$ Variation.

12 wavelengths from the coaxial cable.

The variation in the received power, as the dipole moves within ± two wavelengths of the coaxial cable is shown in Figure 3.2. This figure shows the relative power received at the antenna for various intruder distances from the cable; where the received power is normalized to the maximum power level, the power received when the intruder is at the cable. This curve shows that the received power falls off drastically with distance from the cable; and, that intruder detection would be possible with a very narrow detection region. Figure 3.3 shows the received voltage, again normalized to the value received when the intruder is at the cable, for the probable zone of detection, ± 10 feet or ±0.6 wavelengths.

As noted above, the theoretical calculations indicate the electric field received from the coaxial cable to be negligible; however, Poirier reports that the ambient field, or the field received from the coaxial cable alone, is of the same order magnitude as the maximum field scattered from the intruder-dipole (Ref 9). For this reason, a separate plot, Figure 3.4, was made wherein the field received from the coaxial cable was arbitrarily chosen to be 37% of the field scattered from the dipole when it is located at the coaxial cable, so that a comparison to Poirier's results could be made. In Figure 3.4, the dip occurs when the ambient field and the intruder scattered field are out of

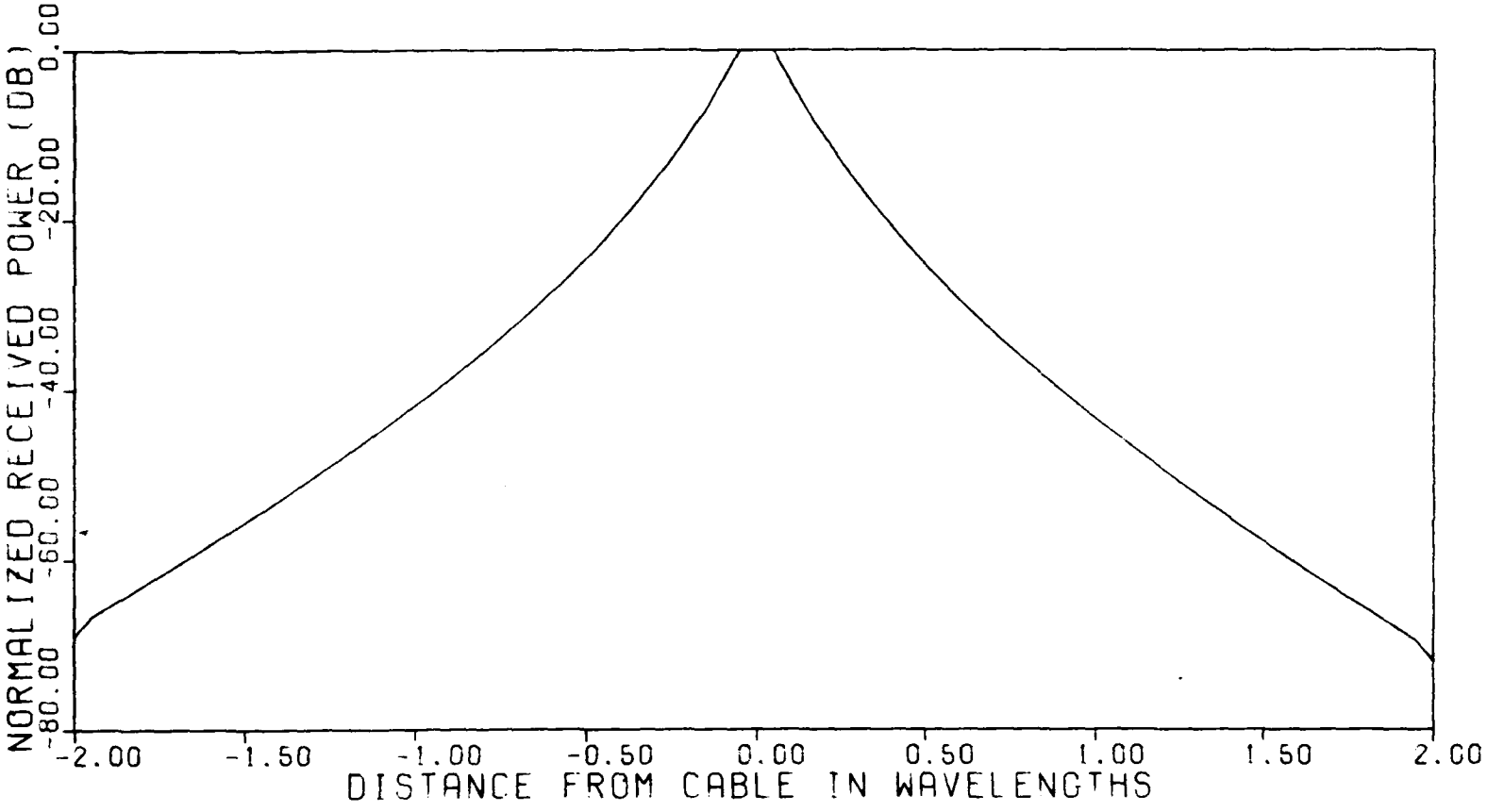

Figure 3.2 Normalized Received Power Variation as an Intruder Moves Along a Radial Path.

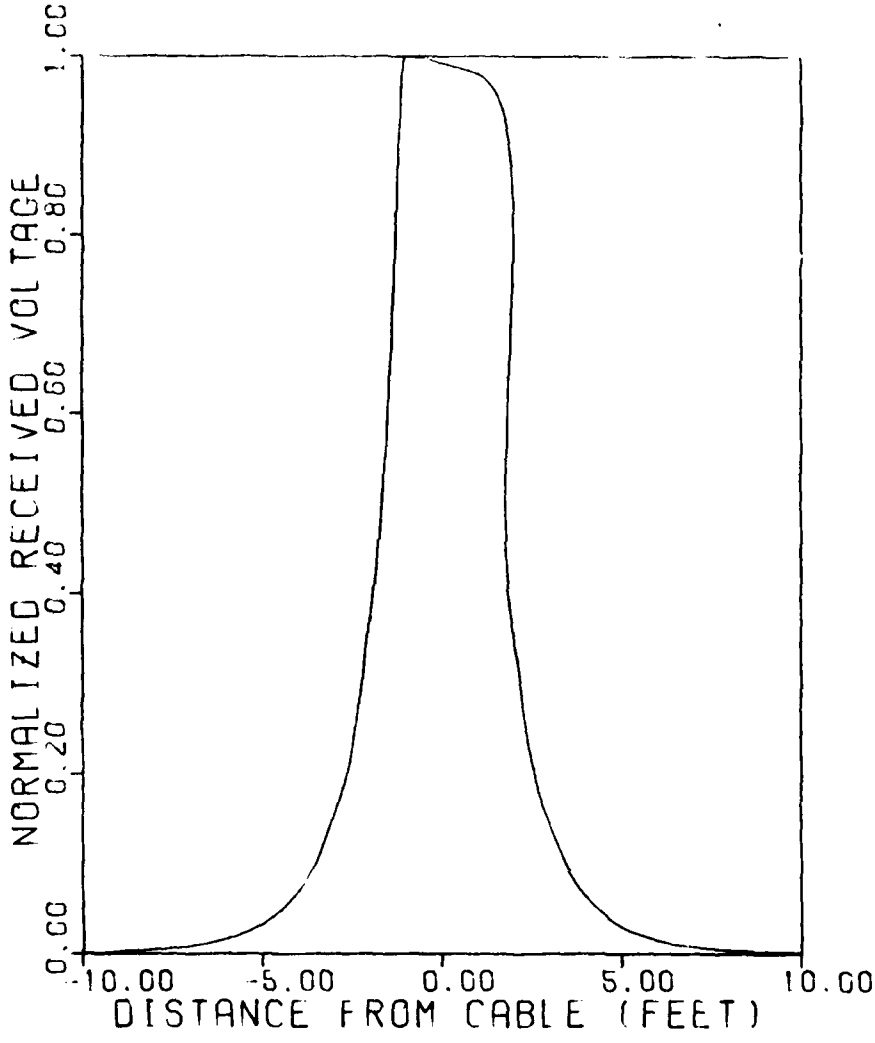

Figure 3.3 Normalized Received Voltage Variation as an Intruder Moves Along a Radial Path. (Note: The "glitch" near the cable is not really there and is due to problems in the plot routine when the dipole is directly over the cable).

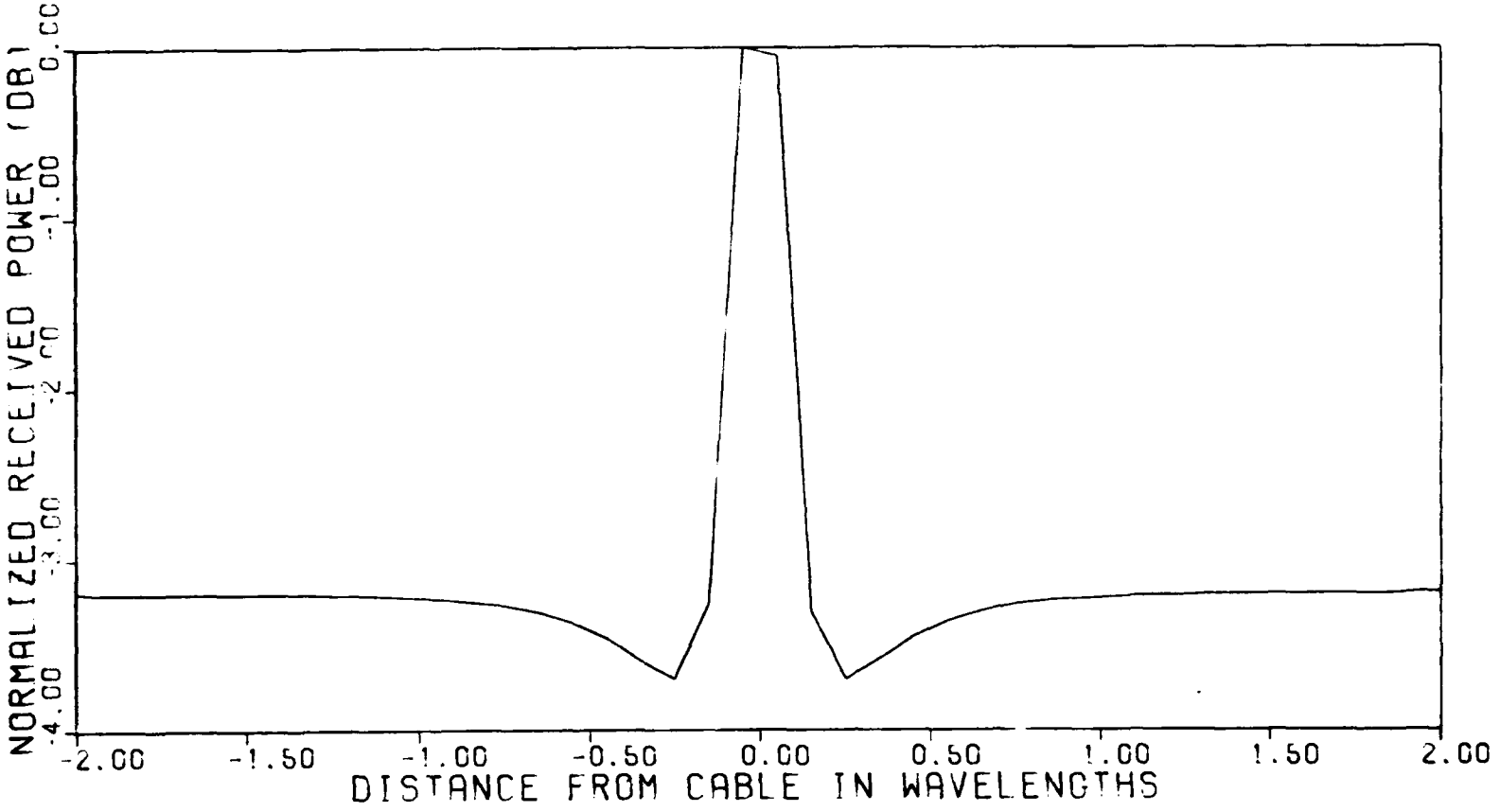

Figure 3.4 Normalized Received Power Variation as an Intruder Moves Along a Radial Path (For the case when Ambient Power = 37% Maximum Intruder Scattered Power).

phase and thus subtract; the peak occurs when they are in phase and the fields add.

3.2 Review of Poirier Report (Ref 8)

Poirier has presented a method for explaining the received field variations due to the interaction between an intruder and the fields produced by the leaky coaxial cable, experimental measurements are also incorporated.

Poirier's approach makes use of the following assumptions/conditions:

1. The coaxial cable is located on the surface of the earth;

2. The earth-air interface does not significantly modify the relative system response (another way of saying free space analysis);

3. The electric field resulting from the leaky coaxial cable is a combination of the coaxial mode and the 'Goubau' mode;

4. The intruder is modeled as a point source located 0.4 meters above the ground; and,

5. The frequency of operation is 75 MHz.

Poirier then goes on to conclude that the power density falls off as $\frac{1}{\rho^2}$ for all ρ's of interest; this conclusion is based on a comparison of the coaxial and 'Goubau' mode power densities with a $\frac{1}{\rho^2}$ decay rate (similar to Figure 3.1), and data reported by Cree and Giles (Ref 3) indicating

that the power decay rate is $\frac{1}{\rho^2}$ for all ρ .

Finally, Poirier makes use of measurements indicating that the ambient electric field, the field received when the intruder is absent, is of the same order magnitude as the field that is scattered from the intruder (Ref 9). So, by letting the total received electric field be the sum of the ambient field and the intruder scattered field, and by normalizing to the ambient field, he obtained the power variation shown in Figure 3.5, which agrees closely with experimental measurements.

3.3 Comparison of Results

Based on the results of sections 3.1 and 3.2, the inescapable conclusion is that a "free space" analysis is incompatible with experimental results which dictate a power decay rate that is primarily determined by $\frac{1}{\rho^2}$. This is further pointed out by realizing that for the point source intruder model, at the point of closest approach, 0.4 meters, Figure 3.1 shows that this is the distance where the power decay rate begins to no longer follow $\frac{1}{\rho^2}$. One can only conclude, that the presence of the earth-air interface somehow enables a form of a bound wave to propagate; possibly accounting for the $\frac{1}{\rho}$ variation instead of the $K_1(\rho)$ variation for the radial electric field component.

Comparison of Figures 3.4 and 3.5 again show that the

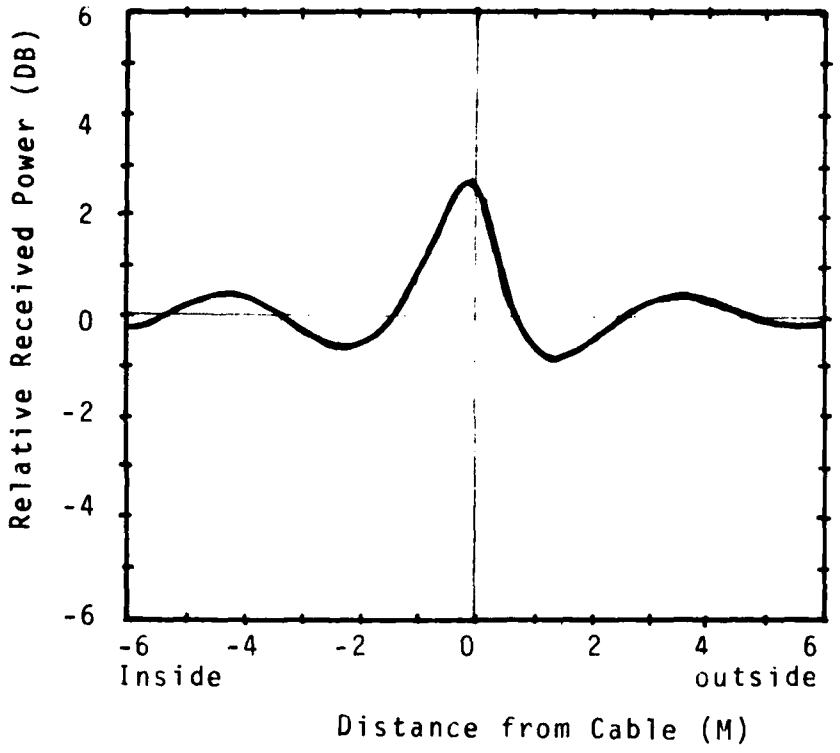

Figure 3.5 Computed Variation of Received Power as an Intruder Moves Along a Radial Path, λ_0 = 4 meters. (From Poirier, Reference 8, Figure 5).

chosen form of the field structure is not correct since the received power, of Figure 3.4, is just the ambient power, except when the intruder is on top of the coaxial cable.

IV. CONCLUSIONS AND RECOMMENDATIONS

4.1 Conclusions

The intent of this investigation was to determine the free space interaction between a dipole and the EM fields created by a leaky coaxial cable. In order to accomplish this, an algorithm for determining the effects of a non-plane wave incident upon a dipole was developed. It was then found that by exciting a current on a dipole, the far field radiation would be greatly enhanced by converting the evanescent field of the coaxial cable into a radiated field from the dipole. However, since this study was undertaken in order to analyze the interaction of an intruder with the EM fields created by a leaky coaxial cable, the following conclusions are made:

1. Intruder detection is possible. The zone of detection is just smaller in the free space case (which may be better).

2. The effects of the earth-air interface cannot be ignored and still obtain exact results. The general character of the response is similar but the ambient levels very significantly.

3. The form of the EM field is apparently affected by the earth-air interface.

4.2 Recommendations

Based on the assumptions stated earlier, and the results presented herein, the following recommendations are made. This problem should be pursued using the approach presented by Van der Pol (Ref 15), with a leaky coaxial cable as the source, in order to determine the proper form of the external EM fields. Another possible reference, using a leaky coaxial cable as the source (Ref 7), could be used in conjunction with Van der Pol to solve the problem of the cable on the earth instead of buried, as done in Reference 7. Once the fields have been properly determined, the computer program developed as part of this study, Appendix A, can be used to determine the interaction with an intruder. Once the proper form of the EM fields are known, it should then be clear what effects the changing environmental conditions would have; this is an extremely important aspect of system performance which needs further investigation.

After the above has been accomplished, one could then begin to determine a more realistic model for the intruder. The modeling of biological bodies for EM radiation has been undertaken by Chen, Livesay and Guru (Ref 2), and by Livesay and Chen (Ref 6).

Bibliography

1. Abramowitz, Milton and Irene A. Stegun. (1964) Handbook of Mathematical Functions. U. S. Government Printing Office, Washington, D.C. (National Bureau of Standards Applied Mathematics, Series 55).

2. Chen, Kun-Mu, Donald E. Livesay, and B.S. Guru. "Induced Current in and Scattered Field from a Finite Cylinder with Arbitrary Conductivity and Permittivity," IEEE Transactions on Antennas and Propagation, Vol AP-24: 330-6 (May 1976).

3. Cree, D.J. and L.J. Giles. "Practical Performance of Radiating Cables," Radio and Electronic Engineer, 45: 221-3 (May 1975).

4. Fernandes, A.S. de C. "Propagation Characteristics of a Loose Braid Coaxial Cable in Free Space," Radio and Electronic Engineer, 49, (5): 255-60 (May 1979).

5. Harrington, Roger F. Time-Harmonic Electromagnetic Fields. New York: McGraw-Hill, 1961.

6. Livesay, Donald E. and Kun-Mu Chen. "Electromagnetic Fields Induced Inside Arbitrarily Shaped Biological Bodies," IEEE Transactions on Microwave Theory and Techniques, Vol MTT-22: 1273-80 (December 1974).

7. Plate, Steven W., David C. Chang, and Edward F. Kuester. Propagating Modes on a Buried Leaky Coaxial Cable. RADC-TR-78-77, interim technical report. Hanscom AFB, Massachusetts: Deputy for Electronic Technology, Hanscom AFB, March 1978. (AD A057 253)

8. Poirier, J.Leon. Estimation of the Zone of Detection of the Single Wire Individual Resource Protection Sensor. RADC-TR-80-258, in house report. Hanscom AFB, Massachusetts: Deputy for Electronic Technology, Hanscom AFB, August 1980. (AD A094 137)

9. --------. (Chief, EM Technical Applications Section, RADC, Hanscom AFB, MA). Private communication.

10. -------- and Martin Kushner. Analysis of the Response of an RF Intruder Protection System. RADC-TR-79-17, in house report. Hanscom AFB, Massachusetts: Deputy for Electronic Technology, Hanscom AFB, January 1979. (AD A072 818)

11. -------- et al. VHF Intrusion Detection: A Technique for Parked Aircraft. RADC-TR-77-384, in house report. Hanscom AFB, Massachusetts: Deputy for Electronic Technology, Hanscom AFB, November 1977. (AD A051 144)

12. Preis, Douglas H. "The Toeplitz Matrix: Its Occurrence in Antenna Problems and a Rapid Inversion Algorithm," IEEE Transactions on Antennas and Propagation, Vol AP-20: 204-6 (March 1972).

13. Rao, K.V.N. et al. "Resource Protection by Segmented Leaky Coax Cables," Proceedings 1979 Carnahan Conference on Crime Countermeasures: 133-7. Lexington, Kentucky: University of Kentucky, May 16-18, 1979.

14. Stutzman, Warren L. and Gary Thiele. Antenna Theory and Design. New York: John Wiley and Sons, 1981.

15. Van der Pol, B. "On Discontinuous Electromagnetic Waves and the Occurrence of a Surface Wave," IRE Transactions on Antennas and Propagation, Vol AP-4: 288-93 (July 1956).

16. Von Hippel, Arthur R. Dielectric Materials and Applications. New York: John Wiley and Sons, 1958.

Appendix A

Developed Computer Program

```
      PROGRAM SWIRPS
C
C     * * * * * * * * * * * * * * * * * * * * * * * * * * * * * * * *
C     *                                                               *
C     *     THIS PROGRAM COMPUTES THE ELECTROMAGNETIC FIELDS          *
C     *     ARISING FROM THE INTERACTION OF A LEAKY COAXIAL CABLE     *
C     *     AND THOSE SCATTERED FROM A DIPOLE.                        *
C     *                                                               *
C     *     THE FIELDS SCATTERED FROM THE DIPOLE ARE CALCULATED       *
C     *     USING THE METHOD OF MOMENTS WITH PULSE FUNCTIONS.         *
C     *                                                               *
C     *     NOTE:  ALL DISTANCES ARE NORMALIZED TO UNITS OF           *
C     *     WAVELENGTHS, AND THUS BECOME DIMENSIONLESS NUMBERS.       *
C     *                                                               *
C     *     LEGEND                                                    *
C     *                                                               *
C     *     AA = LOWER LIMIT OF K-TH ELEMENT                          *
C     *     AB( ) = MIDDLE OF THE K-TH ELEMENT                        *
C     *     ABAR = DIPOLE RADIUS                                      *
C     *     ADIST = DISTANCE FROM COAX TO CENTER OF K-TH ELEMENT      *
C     *     BB = UPPER LIMIT OF K-TH ELEMENT                          *
C     *     BDIST = DISTANCE FROM RECEIVE ANTENNA TO                  *
C     *             CENTER OF K-TH ELEMENT                            *
C     *     BETA = PROPAGATION CONSTANT                               *
C     *     BETA1 = COAXIAL MODE PROPAGATION CONSTANT                 *
C     *           = 1.72 RADS/M                                       *
C     *     BETA2 = 'GOUBAU' MODE PROPAGATION CONSTANT                *
C     *           = 1.32 RADS/M                                       *
C     *     CDIST = DISTANCE FROM RECEIVE ANTENNA TO COAX             *
C     *     CUR( ) = INDUCED CURRENTS                                 *
C     *     C1 = RATIO OF E FIELD FOR COAXIAL/GOUBAU MODES            *
C     *     DDIST( ) = DISTANCE FROM COAX TO INTRUDER                 *
C     *     EDIST = DISTANCE FROM COAX TO CENTER OF KA-TH             *
C     *             ELEMENT OF RECEIVE ANTENNA                        *
C     *     ELBAR = DIPOLE LENGTH                                     *
C     *     EREC( ) = E FIELD AT THE RECEIVE ANTENNA                  *
C     *     ESCAT( ) = E FIELD SCATTERED FROM THE K-TH ELEMENT        *
C     *     K = ELEMENT NUMBER FOR SOURCE ELEMENT                     *
C     *     N = NUMBER OF EXPANSION FUNCTIONS                         *
C     *     PHASE = PHASE DIFFERENCE BETWEEN COAXIAL & GOUBAU MODES   *
C     *     POW( ) = RECEIVED POWER                                   *
C     *     RBAR = DISTANCE FROM SOURCE TO OBSERVATION POINT          *
C     *     TAU( ) = FIRST ROW OR COLUMN OF THE IMPEDENCE MATRIX      *
C     *     U = DISTANCE VARIABLE                                     *
C     *     VIN( ) = INCIDENT E FIELD, VERTICAL COMPONENT             *
C     *     VOLTS( ) = ANTENNA VOLTAGE                                *
C     *     ZINV( ) = INVERTED IMPEDENCE MATRIX                       *
C     *     ZO = CHARACTERISTIC IMPEDENCE (FREE SPACE)                *
C     *     ZOBS = OBSERVATION POINT                                  *
C     *                                                               *
C     * * * * * * * * * * * * * * * * * * * * * * * * * * * * * * * *
C
      COMMON ABAR, BETA, ZOBS, ZJ
      COMPLEX A(100), A1(100), CUR(100), EREC(10), ESCAT(100), TAU(100),
     1        VIN(100), VOLTS(42), ZINV(100,100)
      COMPLEX ADD, AIMONE, CONE, CZERO, FVAL, VMAX, ZIJ, ZJ
      INTEGER COLMN, ROW
```

```
      REAL AB(100), DDIST(42), POW(42)
      REAL K1
      DATA AIMONE/(0.0,1.0)/, CONE/(1.0,0.0)/, CZERO/(0.0,0.0)/
      ABAR=0.005
      C1= 1.0
      CDIST=12.0
      ELBAR=0.355
      IDONE=0
      INVERT=0
      N=100
      PHASE=0.0
      PI=3.14159265358978
      VMAX=CZERO
      ZO=376.7
      ZJ=AIMONE
      BETA=2.0*PI
         BETA1 = 1.72*5.0
          BETA2 = 1.32*5.0
      DEL=ELBAR/N
      ZOBS=ELBAR/(2.0*N)
      DO 90 L=-21,+20,1
      LV = L+ 22
      DDIST(LV) = 0.05 + L/10.0
      DO 20 K=1,N
         IF (IDONE.NE.0) GO TO 15
C        DETERMINE LOWER LIMIT OF K-TH ELEMENT
         AA=ELBAR*(K-1.0)/N
C        DETERMINE UPPER LIMIT OF K-TH ELEMENT
         BB=ELBAR*K/N
C        DETERMINE CENTER OF K-TH ELEMENT
         AB(K)=(AA+BB)/2.0
C
C        COMPUTATION OF IMPEDENCE MATRIX
C
C        PERFORM INTEGRATION USING SIMPSONS RULE. REF "CALCULUS AND
C        ANALYTIC GEOMETRY,2ED", BY JOHN F RANDOLF, PG 427, EQ 5.
         NSTEPS=50
         NN=NSTEPS/2
         DINC=(BB-AA)/NSTEPS
         ADD=CZERO
         U=AA
            DO 10 J=1,NN
            CALL FUNCT(U,FVAL)
            ADD=ADD+2.0*FVAL
            U=U+DINC
            CALL FUNCT(U,FVAL)
            ADD=ADD+4.0*FVAL
            U=U+DINC
10       CONTINUE
C        ADD IN LAST TERM AND CORRECT FIRST TERM
         U=AA
            CALL FUNCT(U,FVAL)
         ADD=ADD-FVAL
         U=BB
            CALL FUNCT(U,FVAL)
         ADD=ADD+FVAL
         ZIJ=ADD*DINC/3.0
```

```
         TAU(K)=ZIJ*ZO/(ZJ*8.0*PI*PI)
15    CONTINUE
C
C        COMPUTATION OF INCIDENT VERTICAL E FIELD
C
         HO=SQRT(BETA1**2.0-BETA**2.0)
          ADIST = SQRT(DDIST(LV)**2.0+ AB(K)**2.0)
         ARG=HO*ADIST
         CALL MODBES(ARG,K1)
         SINEA=AB(K)/ADIST
         VIN(K)=(-2.0*BETA1*K1/(HO*PI))*SINEA
         HO=SQRT(BETA2**2.0-BETA**2.0)
         ARG=HO*ADIST
         CALL MODBES(ARG,K1)
         VIN(K)=VIN(K)-2.*BETA2*K1*SINEA*CEXP(-ZJ*PHASE)/(HO*PI*C1)
20    CONTINUE
      IDONE=1
C
C        COMPUTATION OF Z-INVERSE
C
      IF (INVERT.NE.0) GO TO 30
      INVERT=1
      NZ=N
      CALL TOPINV(TAU,NZ,A,A1,ZINV)
30    CONTINUE
C
C        COMPUTATION OF INDUCED CURRENT
C
      DO 50 ROW=1,N
         CUR(ROW)=CZERO
         DO 40 COLMN=1,N
            CUR(ROW)=CUR(ROW)+ZINV(ROW,COLMN)*VIN(COLMN)
40       CONTINUE
50    CONTINUE
C
C        DETERMINE THE VERTICAL E FIELD AT ANTENNA DUE TO COAX
C
      DO 60 KA=1,10
         ANT=KA/10.0-0.05
         PHI=ATAN(ANT/CDIST)
         EDIST=SQRT(ANT**2.0+CDIST**2.0)
         HO=SQRT(BETA1**2.0-BETA**2.0)
         ARG1=HO*EDIST
         CALL MODBES(ARG1,K1)
         EREC(KA)=(-2.0*BETA1*K1/(HO*PI))*SIN(PHI)
         HO=SQRT(BETA2**2.0-BETA**2.0)
         ARG1=HO*EDIST
         CALL MODBES(ARG1,K1)
      EREC(KA) = (-2.0*BETA2*K1/(HO*PI*C1))*SIN(PHI)*CEXP(-ZJ*PHASE)
     1           + EREC(KA)
60    CONTINUE
C
C        COMPUTATION OF THE SCATTERED VERTICAL E FIELD AT THE ANTENNA
C        FROM THE K-TH ELEMENT AND THE RESULTING RECEIVED E FIELD
C
      VOLTS(LV) = CZERO
      DO 80 K=1,N
```

```
         DO 70 KA=1,10
            ANT=KA/10.0-0.05
            DIF=ABS(AB(K)-ANT)
            BDIST=SQRT(DIF**2.0+(CDIST+DDIST(LV))**2.0)
            GAMMA=ASIN(AB(K)/BDIST)
            THETA=GAMMA+PI/2.0
            ESCAT(K)=ZJ*CUR(K)*DEL*ZO*SIN(THETA)*CEXP(-ZJ*BETA*BDIST)/
     1              (2.0*BDIST)
            CHI=ATAN(DIF/(CDIST+DDIST(LV)))
            EREC(KA)=EREC(KA)-ESCAT(K)*COS(CHI)
         VOLTS(LV) = VOLTS(LV) + 0.01*EREC(KA)
70          CONTINUE
80       CONTINUE
         IF (CABS(VOLTS(LV)) .GT. CABS(VMAX))   VMAX = VOLTS(LV)
90       CONTINUE
         DO 100 LP=1,42
         POW(LP) = 10.0*LOG10((CABS(VOLTS(LP))/CABS(VMAX))**2.0)
100      CONTINUE
         PRINT'(T5,A,T20,A)','INTRUDER','RECEIVED'
         PRINT'(T5,A,T21,A)','DISTANCE','POWER'
         PRINT'(T7,F5.2,T20,F7.2)',(DDIST(MD),POW(MD),MD=1,42)
         STOP
         END

         SUBROUTINE TOPINV(TAU,NZ,A,A1,ZINV)
C
C        * * * * * * * * * * * * * * * * * * * * * * * * * * * * * * * *
C        *                                                               *
C        *     THIS SUBROUTINE DETERMINES THE INVERSE OF A TOEPLITZ      *
C        *     MATRIX WHEN GIVEN EITHER THE FIRST ROW OR COLUMN OF THE   *
C        *     TOEPLITZ MATRIX.                                          *
C        *                                                               *
C        *     NOTE:  THIS ROUTINE IS MORE EFFICIENT THAN A GENERAL      *
C        *     MATRIX INVERSION ROUTINE BECAUSE IT MAKES USE OF THE      *
C        *     SPECIAL PROPERTIES OF A TOEPLITZ MATRIX.                  *
C        *                                                               *
C        *     THIS SUBROUTINE IS A MODIFICATION OF SUBROUTINE TPLZ      *
C        *     FROM      "ANTENNA THEORY AND DESIGN"                     *
C        *     BY        STUTZMAN AND THIELE, PAGE 579 - 81.             *
C        *                                                               *
C        *     LEGEND                                                    *
C        *                                                               *
C        *     A,A1 = SCRATCH AREA VECTORS OF LENGTH NZ                  *
C        *     IER  = ERROR CODE, EQUAL TO ZERO IF MATRIX IS INVERTIBLE  *
C        *     NZ   = ORDER OF THE TOEPLITZ MATRIX                       *
C        *     TAU  = FIRST ROW OR COLUMN OF THE TOEPLITZ MATRIX         *
C        *     ZINV = THE INVERTED TOEPLITZ MATRIX                       *
C        *                                                               *
C        * * * * * * * * * * * * * * * * * * * * * * * * * * * * * * * *
C
         COMMON ABAR, BETA, ZOBS, ZJ
         COMPLEX A(NZ), A1(NZ), TAU(NZ), ZINV(NZ,NZ)
         COMPLEX ALMDA, ALPHA, C1, C2, COEF, CONE, CZERO, FAC, TAU1
         DATA CONE/(1.0,0.0)/, CZERO/(0.0,0.0)/
         N=NZ-1
         IER=0
         TAU1=TAU(1)
         DO 2000 II=1,N
```

```
2000  TAU(II)=TAU(II+1)/TAU1
      ALMDA=CONE-TAU(1)*TAU(1)
      A(1)=-TAU(1)
      I=2
1     KK=I-1
      ALPHA=CZERO
      DO 2 M=1,KK
      LL=I-M
2     ALPHA=ALPHA+A(M)*TAU(LL)
      ALPHA=-(ALPHA+TAU(I))
      IF (CABS(ALPHA).EQ.0.00) GO TO 15
      COEF=ALPHA/ALMDA
      ALMDA=ALMDA-COEF*ALPHA
      DO 3 J=1,KK
      L=I-J
3     A1(J)=A(J)+COEF*A(L)
      DO 7 J=1,KK
7     A(J)=A1(J)
      A(I)=COEF
      IF (I.GE.N) GO TO 5
4     I=I+1
      GO TO 1
5     NH=(NZ+1)/2
      FAC=ALMDA*TAU1
      NP=NZ+1
      DO 51 I=1,NH
      IF (I.NE.1) GO TO 52
      A1(1)=CONE/FAC
      DO 53 J=2,NZ
      A1(J)=A(J-1)/FAC
53    CONTINUE
      GO TO 54
52    CONTINUE
      JH=I-1
      C1=A(JH)
      NNPI=NP-I
      C2=A(NNPI)
      DO 55 JJ=1,N
      J=NP-JJ
      INPJ=NP-J
      JL=J-1
      A1(J)=A1(JL)+(C1*A(JL)-C2*A(INPJ))/FAC
55    CONTINUE
      A1(1)=A(I-1)/FAC
54    CONTINUE
      DO 57 J=1,NZ
      ZINV(I,J)=A1(J)
      KNPJ=NP-J
      KNPI=NP-I
      ZINV(KNPI,J)=A1(KNPJ)
57    CONTINUE
51    CONTINUE
      RETURN
15    PRINT*,'ERROR HAS OCCURRED. MATRIX IS NOT STRONGLY NONSING'
      IER=I
      RETURN
      END
```

```
      SUBROUTINE FUNCT(U,FVAL)
C
C     * * * * * * * * * * * * * * * * * * * * * * * * * * * * * * * * *
C     *                                                               *
C     *     THIS SUBROUTINE COMPUTES THE VALUE OF THE FUNCTION BEING  *
C     *     INTEGRATED IN EQUATION 2.23.                              *
C     *                                                               *
C     * * * * * * * * * * * * * * * * * * * * * * * *   * * * * * * *
C
      COMMON ABAR, BETA, ZOBS, ZJ
      COMPLEX A1, FVAL, ZJ
      UTOZ=U-ZOBS
      RBAR=SQRT(ABAR**2.0+UTOZ**2.0)
      A1=(2.0*RBAR**2.0-3.0*ABAR**2.0)*(1.0+ZJ*BETA*RBAR)
      A2=(BETA*RBAR*ABAR)**2.0
      FVAL=(CEXP(-ZJ*BETA*RBAR)*(A1+A2))/(RBAR**5.0)
      RETURN
      END

      SUBROUTINE MODBES(X,K1)
C
C     * * * * * * * * * * * * * * * * * * * * * * * * * * * * * * * * *
C     *                                                               *
C     *     THIS SUBROUTINE DETERMINES THE VALUE OF THE MODIFIED      *
C     *     BESSEL FUNCTION OF THE SECOND KIND, ORDER ONE, GIVEN      *
C     *     A REAL ARGUMENT                                           *
C     *                                                               *
C     *     LEGEND                                                    *
C     *                                                               *
C     *     I1    = MODIFIED BESSEL FCTN OF THE FIRST KIND, ORDER ONE *
C     *     K1    = MODIFIED BESSEL FCTN OF THE SECOND KIND, ORDER ONE*
C     *     X     = REAL ARGUMENT                                     *
C     *                                                               *
C     * * * * * * * * * * * * * * * * * * * * * * * * * * * * * * * * *
C
      REAL I1,K1
      IF (X.GE.2.0) GO TO 1000
C        REFERENCE:  ABRAMOWITZ, EQS 9.8.3 & 9.8.7, PGS 378-9.
      T=X/3.75
      I1=X*(0.5+0.87890594*T**2.0+0.51498869*T**4.0+0.15084934*T**6.0+
     10.02658733*T**8.0+0.00301532*T**10.0+0.00032411*T**12.0)
      K1=(1.0/X)*(X*LOG(X/2.0)*I1+1.0+0.15443144*(X/2.0)**2.0-0.67278579
     1*(X/2.0)**4.0-0.18156897*(X/2.0)**6.0-0.01919402*(X/2.0)**8.0-
     20.00110404*(X/2.0)**10.0-0.00004686*(X/2.0)**12.0)
      RETURN
1000  CONTINUE
C        REFERENCE:  ABRAMOWITZ, EQS 9.8.8, PGS 379.
      Y=EXP(X)*SQRT(X)
      YY=1.0/Y
      K1=( YY )*(1.25331414+0.23498619*(2.0/X)-0.03655620*(2.0/X)**2.0+
     10.01504268*(2.0/X)**3.0-0.00780353*(2.0/X)**4.0+0.00325614*(2.0/X)
     2**5.0-0.00068245*(2.0/X)**6.0)
      RETURN
      END
```

VITA

Daryl L. Tomczyk was born on 15 December 1949 in Denver, Colorado. He graduated from high school in Denver, Colorado in 1968 and attended Colorado State University from which he received the degree of Bachelor of Science in Electrical Engineering in June 1972. Upon graduation he was employed as a marketing engineer for Motorola Semiconductor Products Division, Mesa, Arizona. He entered the Air Force on active duty in January 1978, and received his commission from Officer Training School in April 1978. He served as a Nuclear Effects Test Officer with the Air Force Weapons Laboratory at Kirtland AFB, New Mexico, until entering the School of Engineering, Air Force Institute of Technology, in June 1980.

Permanent address: 1330 151st Place NE
Bellevue, Washington 98007

UNCLASSIFIED
SECURITY CLASSIFICATION OF THIS PAGE *(When Data Entered)*

REPORT DOCUMENTATION PAGE	READ INSTRUCTIONS BEFORE COMPLETING FORM
1. REPORT NUMBER: AFIT/GE/EE/81D-60	2. GOVT ACCESSION NO.: AD-A115 535
3. RECIPIENT'S CATALOG NUMBER:	
4. TITLE *(and Subtitle)*: FREE SPACE ANALYSIS OF THE SCATTERED ELECTROMAGNETIC FIELDS AS A DIPOLE APPROACHES A LEAKY COAXIAL CABLE	5. TYPE OF REPORT & PERIOD COVERED: MS Thesis
	6. PERFORMING ORG. REPORT NUMBER:
7. AUTHOR(s): Daryl L. Tomczyk, 1Lt. USAF	8. CONTRACT OR GRANT NUMBER(s):
9. PERFORMING ORGANIZATION NAME AND ADDRESS: Air Force Institute of Technology(AFIT-EN) Wright-Patterson AFB, Ohio 45433	10. PROGRAM ELEMENT, PROJECT, TASK AREA & WORK UNIT NUMBERS:
11. CONTROLLING OFFICE NAME AND ADDRESS: Electromagnetic Technical Applications Sec. Rome Air Development Center RADC/EECS Hanscom AFB, Massachusetts	12. REPORT DATE: December 1981 13. NUMBER OF PAGES: 58
14. MONITORING AGENCY NAME & ADDRESS *(if different from Controlling Office)*:	15. SECURITY CLASS. *(of this report)*: UNCLASSIFIED 15a. DECLASSIFICATION DOWNGRADING SCHEDULE:

16. DISTRIBUTION STATEMENT *(of this Report)*
Approved for public release; distribution unlimited.

17. DISTRIBUTION STATEMENT *(of the abstract entered in Block 20, if different from Report)*

15 APR 1982
Dean for Research and Professional Development
Air Force Institute of Technology (ATC)
Wright-Patterson AFB, OH 45433

18. SUPPLEMENTARY NOTES
Approved for public release; IAW AFR 190-17
FREDERIC C. LYNCH, Major, USAF
Director of Public Affairs

19. KEY WORDS *(Continue on reverse side if necessary and identify by block number)*
Intrusion Detectors
Coaxial Cables
Electromagnetic Fields
Electromagnetic Scattering

20. ABSTRACT *(Continue on reverse side if necessary and identify by block number)*
The free space interaction of the near zone electromagnetic fields external to a leaky coaxial cable and a moving dipole is investigated. The method of moments and the equivalence principle are used to find the currents on the dipole and the electromagnetic fields scattered from the dipole. Finally, the overall interaction between these two fields is determined by superposition. The theoretically derived results are then compared with experimental

DD FORM 1 JAN 73 1473 EDITION OF 1 NOV 65 IS OBSOLETE

UNCLASSIFIED
SECURITY CLASSIFICATION OF THIS PAGE *(When Data Entered)*

measurements.

The findings of this report indicate that exact results are not obtained with a free space analysis; therefore, further work involving electronic intruder detection analysis should include the effects of the earth-air interface.